Journal of Catalysis **208,** 291–300 (2002)
doi:10.1006/jcat.2002.3586

Methanol Decomposition on Cu(111): A DFT Study

Jeff Greeley and Manos Mavrikakis[1]

Department of Chemical Engineering, University of Wisconsin—Madison, Madison, Wisconsin 53706

Received July 17, 2001; revised March 3, 2002; accepted March 3, 2002

Self-consistent periodic DFT–GGA calculations are used to investigate the methanol decomposition pathway on both equilibrium and stretched Cu(111) surfaces. The thermochemistry and kinetics of the decomposition via sequential hydrogen abstraction are both found to be highly unfavorable. The second step in this pathway, the abstraction of hydrogen from the methoxy intermediate, has large thermochemical (∼0.6 eV) and kinetic (∼1.4 eV) barriers. Our thermochemical results indicate that methanol, formaldehyde, and carbon monoxide are weakly bound to the surface and will likely desorb before undergoing any reaction under UHV conditions. In contrast, methoxy, formyl, and atomic hydrogen are much more strongly bound. Introduction of a 4% lateral strain to the Cu(111) lattice decreased the transition state energy of the methoxy hydrogen abstraction step, suggesting that strain might facilitate the kinetics of this reaction. © 2002 Elsevier Science (USA)

Key Words: **density functional theory; catalysis; surface stress; copper; methanol; formaldehyde; formyl; carbon monoxide.**

INTRODUCTION

The decomposition pathway of methanol on copper, and in particular the elementary step in this pathway that involves the dehydrogenation of methoxy to formaldehyde, plays an important role in the *methanol steam reforming* process. This process, which occurs over an Al_2O_3-supported Cu/ZnO catalyst, has the potential to provide an economical, convenient source of hydrogen for next-generation fuel cells. The methanol steam reforming process is actually a composite process involving methanol decomposition, the reaction of methanol with water, and the water–gas shift reaction. Peppley *et al.* (1) created a microkinetic model of this process incorporating all three of these reaction pathways and determined that the rate-limiting step of both the reaction of methanol with water and the methanol decomposition reaction is the dehydrogenation of adsorbed methoxy to formaldehyde. A detailed understanding of this step is, therefore, crucial to accurate modeling of the steam reforming process and is a major motivation for this study.

[1] To whom correspondence should be addressed. Fax: (608) 262-5434. E-mail: manos@engr.wisc.edu.

An additional motivation for studying the process of methanol decomposition on copper (with a focus on the methoxy dehydrogenation step) is to probe certain elementary steps that occur during the *methanol synthesis* process. Methanol, with a worldwide demand of 8.94 billion gallons in 1999 (2), is one of the most important synthetic chemicals on the market today. Methanol is synthesized by hydrogenation of a CO and CO_2 mixture over Al_2O_3-supported Cu/ZnO (3, 4). The methanol synthesis process can be thought of in terms of two major pathways. The first, which starts with CO, is essentially the microscopic reverse of the methanol decomposition pathway. The second, starting with CO_2, is the microscopic reverse of methanol reforming with water. The former pathway is almost kinetically insignificant compared to the latter pathway. ^{14}C labeling experiments have shown that, via the formation of a formate intermediate, CO_2 provides the main source of carbon for methanol synthesis from $H_2/CO/CO_2$ feeds over Al_2O_3-supported Cu/ZnO (5, 6). Nerlov and Chorkendorff (7) measured a zero rate of reaction for H_2/CO over Cu(100). Finally, Askgaard *et al.* (3) created a kinetic model of methanol synthesis that neglected the CO pathway and still obtained very good agreement with experimental results. In spite of the fact that the CO pathway is not the primary pathway of methanol synthesis, this pathway is worthy of first-principles study as a reference point for a study of the more complicated methanol/water reaction pathway. In addition, certain steps late in the CO pathway (e.g., the hydrogenation of formaldehyde to methoxy in the presence of surface oxygen) may play a significant kinetic role in methanol synthesis. It has been proposed, for example, that formaldehyde might form via dioxymethylene decomposition during methanol synthesis over Cu(100) (8). The formaldehyde may then be hydrogenated to methoxy in a kinetically significant reaction pathway.

A final industrial reaction that motivates this study is the *partial oxidation of methanol to formaldehyde* that occurs over silver. In 1999, 35% of the worldwide production of methanol was used to produce formaldehyde through this and through an iron molybdate process (2, 9). The broad chemical features of methanol partial oxidation on silver and copper are similar (10, 11). Thus, although it is not directly comparable to studies of methanol oxidation on

0021-9517/02 $35.00

silver (a noble metal), the first-principles study of methanol decomposition on copper (another noble metal) can be considered as a first step toward an improved understanding of the former process.

The methanol decomposition process has been the focus of considerable research effort in the past 20 years. Although methanol is not significantly adsorbed on copper under normal methanol synthesis conditions, it is found to adsorb molecularly on most low-index copper surfaces under UHV conditions at low temperatures. To facilitate methanol decomposition, single crystal surfaces are generally *predosed* with *oxygen*. In TPD experiments, most of this oxygen desorbs as water before further decomposition of methoxy occurs. Single-crystal studies of this type, some with and some without oxygen predosing, have been performed on Cu(100) (7, 8, 12), Cu(110) (11, 13–16), and Cu(111) (17). Higher pressure TPD studies on polycrystalline copper (with some evidence for the presence of trace amounts of adsorbed oxygen) have been performed as well (18, 19). Finally, EXAFS and XAS have been used to study methanol oxydehydrogenation on polycrystalline surfaces under industrial reaction conditions (20–23).

On many transition metals, methanol decomposition proceeds through successive formation of methoxy, formaldehyde, formyl, CO, and hydrogen (for a review, see 24). The decomposition mechanism on Cu(111) appears to be similar; studies of the reactants, products, and intermediates involved in methanol decomposition on this surface are numerous. More specifically, the *methoxy* intermediate on Cu(111) has been studied in great detail by many researchers. Experimental investigations have been undertaken with NEXAFS, XPD, HREELS, and ARPS (25–30), and theoretical cluster calculations (using between 3 and 25 metal atoms) have been performed with HF-LCAO, MO-SCF, and DFT methods (31–34). Less information is available about the interaction of *formaldehyde* with the Cu(111) surface. Experimental studies are difficult because formaldehyde easily polymerizes on metal surfaces (35), thereby obscuring information about the behavior of isolated formaldehyde molecules. Theoretical studies are also challenging because of the weakly adsorbed state of formaldehyde on Cu(111) (36, 37). As is the case with formaldehyde, the *formyl* radical on transition metal surfaces has not been well studied. Gomes and Gomes (38) performed DFT cluster calculations on Cu(111), Yang (39) performed all-electron calculations for the radical on Ni(111), and Yates and Cavanagh (40) used TIS to examine formyl on supported rhodium. *Carbon monoxide* on Cu(111) has been studied both experimentally (see, e.g., 41, 42) and theoretically (43). *Hydrogen* on Cu(111) has also been reasonably well studied. Experimental investigations of the dissociation of H_2 on the surface are numerous (see, e.g., 44), and many theoretical studies have also been performed (e.g., 45).

The role of surface *strain* in the chemical kinetics and thermochemistry of surface reactions has received considerable attention in the recent literature. Strain can be present in pseudomorphic metallic overlayers (46–48), in thin, supported, metal particles (49), or around unrelaxed surface defects such as dislocations (50). Strain has been shown to have a substantial effect on the kinetics and thermochemistry of the reactions of simple adsorbates such as O and CO (51, 52). It has also been suggested that strain plays a role in methanol synthesis and in the partial oxidation of methanol on copper catalysts (20–23, 53).

In this study, we perform a periodic self-consistent DFT investigation of the methanol decomposition pathway on Cu(111). This pathway involves sequential abstractions of hydrogen atoms from methanol to yield CO and H_2. We investigate the thermochemistry of each elementary step, and we study the full reaction path of the second step in the pathway, the abstraction of a single hydrogen atom from methoxy, to identify the transition state for this elementary step. Experimentally, it has been demonstrated that this is a likely candidate for the rate-limiting step of the methanol decomposition reaction (1, 17). We extend the analysis of this elementary reaction step to a stretched Cu(111) surface. Finally, we compare our results with previous experimental and theoretical studies of the methanol decomposition process and discuss the possible role of surface defects, strain, and surface oxygen in this process.

METHODS

DACAPO, the total energy calculation code developed by Nørskov and coworkers (54), is used for all calculations in this study. A three-layer slab representing Cu(111), periodically repeated in a super cell geometry with five equivalent layers of vacuum between any two successive metal slabs, is used. Detailed thermodynamic calculations are performed on 2×2 (surface coverage of 1/4 ML) and 3×3 (surface coverage of 1/9 ML) unit cells. Hydrogen abstraction calculations are all performed on a 3×3 unit cell. Coverages in this range are typical of methanol synthesis catalysts operating at pressures of $\sim$50 atm; a detailed microkinetic model of the reaction at this pressure predicts, for example, that vacant surface sites account for over half of all available sites, atomic hydrogen occupies one-third of the sites, and methanol occupies only 4% of the sites (3). Adsorption is allowed on only one of the two surfaces exposed and the electrostatic potential is adjusted accordingly (55).

All of the atoms in the slab are kept fixed at their bulk-truncated positions (the effect of surface relaxation on all binding energies is found to be less than 0.05 eV). Ionic cores are described by ultrasoft pseudopotentials (56), and the Kohn–Sham one-electron valence states are expanded in a basis of plane waves with kinetic energy below 25 Ry. The surface Brillouin zone is sampled at 18 special **k** points.

In all cases, convergence of the total energy with respect to the **k** point set and with respect to the number of metal layers included is confirmed. The exchange-correlation energy and potential are described by the generalized gradient approximation (GGA-PW91) (57, 58). The self-consistent PW91 density is determined by iterative diagonalization of the Kohn–Sham Hamiltonian, Fermi population of the Kohn–Sham states ($k_BT = 0.1$ eV), and Pulay mixing of the resulting electronic density (59). All total energies have been extrapolated to $k_BT = 0$ eV.

The calculated PW91 bond energy for $H_2(g)$ is 4.57 eV, in reasonable agreement with the experimental value of 4.52 eV at 298 K (60). The lattice constant for bulk Cu is found to be 3.66 Å, in good agreement with the experimental value of 3.615 Å (60). In the calculations for stretched surfaces, the lattice constant is increased by ~4% to 3.80 Å. The lattice is stretched in both directions of the surface plane, but the direction perpendicular to the surface plane is kept at its bulk, equilibrium separation. This approach has been shown to give a good estimate of the effect of strain on the thermochemistry and kinetics of surface reactions on transition metal surfaces (52).

The reaction path of hydrogen abstraction from methoxy is studied based on the assumption that the C–H bond length represents a good approximation to the actual reaction coordinate. Given the weak site preferences of all species involved, the initial and final states are chosen for maximum symmetry of the path. The methoxy radical (the reactant) is placed in an fcc site, the hydrogen product in an hcp site, and the formaldehyde product in an η_2-type site with the C–O bond axis parallel to the bridge site between the fcc and hcp sites in question. A linear path is interpolated between the reactant and the products, and five configurations on this path are analyzed. The carbon–hydrogen bond length is fixed for each of these configurations, and all other ionic degrees of freedom are allowed to relax. An approximate criterion is used to identify the transition state; namely, the projected force along the C–H bond axis is assumed to go from attractive to repulsive as the system moves through the transition state. The transition state is thus taken to be the configuration in which the projected force is zero. Subsequent calculations performed with this approximate method for determining a reaction path and with the more sophisticated nudged elastic band (NEB) method (61, 62) for methanol decomposition on Pt(111) (63) show that the results of these two methods are fairly close to each other.

RESULTS

Structure and Energetics of Adsorbed Intermediates

A brief overview of the major thermochemical results is given in this section. Site preferences and binding energies (more negative energies indicate more stable configurations) for the intermediates in our investigation are described for 1/9-ML surface coverage. The description focuses primarily on the most favorable binding configurations for the adsorbates, but data on the best three configurations for each adsorbate are given in Table 1. Schematics and geometrical information for the best configurations are shown in Figs. 1a and 1b, and schematics of some of the less favorable configurations are presented in Fig. 1c. A brief mention of coverage effects on binding energies and site preferences concludes this section.

TABLE 1

Binding Energies of Methanol Decomposition Intermediates on Cu(111)

Adsorbate	Binding configuration	Binding energy (eV)
Methanol	O–H top–bridge–top	−0.16
	O–H top-hcp	−0.14
	fcc	−0.13
Methoxy	fcc, C–O perp. to surface	−2.08
	hcp, C–O perp. to surface	−2.02
	bridge, C–O perp. to surface	−1.90
Formaldehyde	top–bridge–top (disigma)	−0.10
	bridge	−0.10
	π-Bonded	−0.10
Formyl	top–bridge–top	−1.15
	HhCbOft	−1.13
	HbChOht	−1.13
Carbon monoxide	fcc	−0.79
	hcp	−0.78
	bridge	−0.72
Atomic hydrogen	fcc	−2.37
	hcp	−2.37
	bridge	−2.23

Note. θ = 1/9 ML. Negative numbers indicate stable intermediates. Energy reference corresponds to adsorbate and slab at infinite separation between each other.

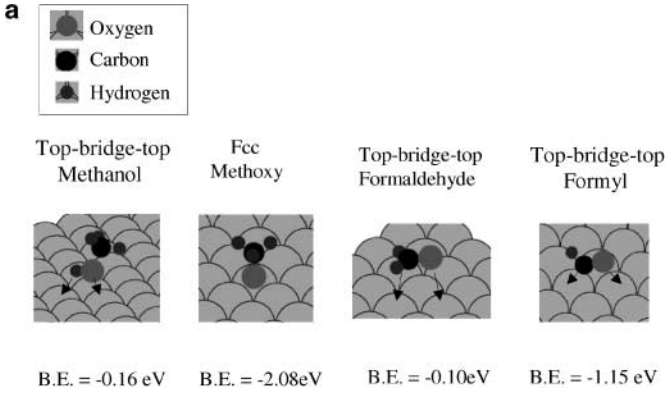

FIG. 1a. The most stable configurations for methanol decomposition intermediates on Cu(111). Negative numbers indicate stable intermediates. Energy reference corresponds to adsorbate and slab at infinite separation between each other. B.E. denotes binding energy.

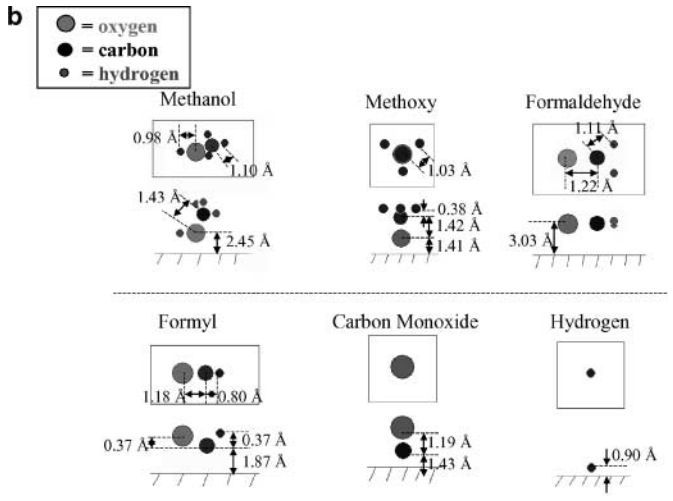

FIG. 1b. Calculated structural data for the most stable states of methanol decomposition intermediates on Cu(111). *Top views* of adsorbates are given immediately after adsorbate name, followed by slab *cross sections*.

Methanol is found to be weakly bound to the Cu(111) surface. The best configuration appears to involve an O–H bond that is roughly parallel to the surface in a top–bridge–top configuration (Fig. 1a). Quantitative geometrical information about this configuration is given in Fig. 1b, and a binding energy of −0.16 eV is calculated (Table 1). It is interesting that the preference for this configuration appears to be relatively weak, as evidenced by the near degeneracy of other adsorbed methanol states with this state (Table 1, Fig. 1c).

For the *methoxy* radical, a strong energetic preference for threefold sites is found. The best configuration (an fcc site with the C–O bond perpendicular to the surface—Figs. 1a and 1b) is found to have a binding energy of −2.08 eV (Table 1). Although the methoxy generally seems to adsorb with the C–O bond perpendicular to the Cu(111) surface, stable configurations with tilted C–O orientations do exist. We find two such configurations at fcc sites, both with C–O angles of approximately 5° to the surface normal. These configurations differ energetically by less than 0.02 eV from the perpendicular configurations. Rotation of the methoxy about the C–O bond in the threefold sites has a very small effect on the total energy. The energy is found to increase by only about 0.03 eV when the methoxy hydrogen atoms are rotated from an overbridge configuration to an overtop configuration.

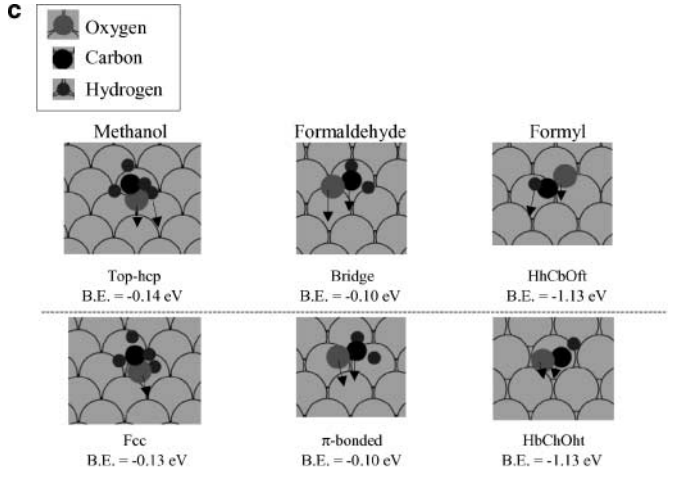

FIG. 1c. The second and third most stable configurations for methanol decomposition intermediates on Cu(111). Negative numbers indicate stable intermediates. Energy reference corresponds to adsorbate and slab at infinite separation between each other. B.E. denotes binding energy. HhCbOft indicates that H is above an hcp site, C is above a bridge site, and O is between an fcc and a top site.

Formaldehyde binds weakly to the Cu(111) surface. The preferred binding mode seems to be an η_2 configuration with the C–O bond roughly parallel to the surface. The oxygen atom is found to point slightly away from the surface. The most favorable configuration is a disigma (top–bridge–top) state with the oxygen and carbon atoms approximately 3.5 Å above the surface (Figs. 1a and 1b); a binding energy of −0.10 eV is found for this state. As was the case with methanol, the preference for this state is weak, and several degenerate or near-degenerate configurations are present (Table 1, Fig. 1c).

The *formyl* radical binds preferentially in a top–bridge–top configuration (Figs. 1a and 1b) with a binding energy of −1.15 eV; additional near-degenerate states exist (Table 1, Fig. 1c). *Carbon monoxide* binds through the carbon atom at a threefold fcc site (Fig. 1b) with a binding energy of −0.79 eV; the hcp site has a comparable energy (Table 1). Like methoxy, *atomic hydrogen* prefers threefold sites on Cu(111). The most stable configuration is found at an fcc site (Fig. 1b) although the hcp site is quasidegenerate to the fcc. A binding energy of −2.37 eV is obtained (Table 1).

The effect of changing *coverage* on the above thermochemical results has been briefly analyzed for the adsorbates described above. The results indicate that in changing the coverage from 1/9 to 1/4 ML, the absolute binding energies can change by as much as 10%, but binding energy differences (between different configurations of the same adsorbate) change by only a few hundredths of an electron volt. Such small changes are within the error bars of this type of calculation. Hence, we are unable to meaningfully calculate any coverage-induced changes in site preference, and we neglect this effect in our analyses in this paper.

Hydrogen Abstraction from Methoxy

We analyze the reaction barrier of the second step of the methanol decomposition pathway (the abstraction of hydrogen from methoxy). Results for the equilibrium Cu(111) surface are presented here (Fig. 2), and corresponding results for the stretched surface (Fig. 3) are analyzed in the discussion section. The 3×3 unit cell used in our calculations

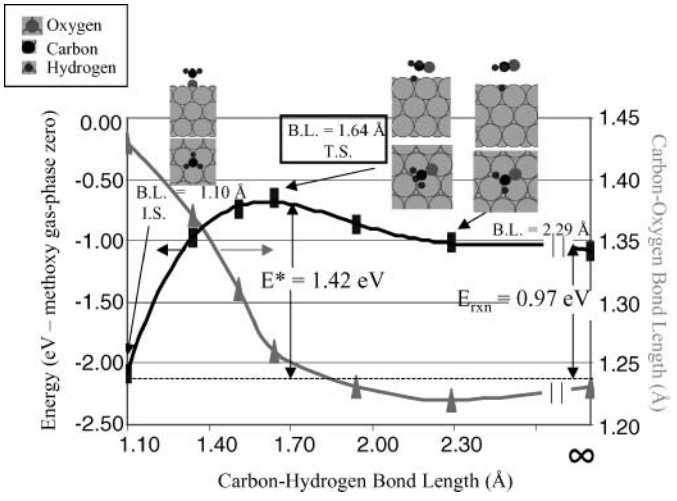

FIG. 2. Reaction coordinate for hydrogen abstraction from methoxy on Cu(111). Line connecting rectangles corresponds to energy. Line connecting triangles corresponds to carbon-oxygen bond length (for reference, the gas-phase O-CH_2 B.L. is 1.22 Å). B.L. denotes carbon–hydrogen bond length. I.S. denotes initial state. T.S. denotes transition state. Diagrams include slab cross sections and top views. Zero of energy corresponds to a gas-phase methoxy at infinite separation from the slab. The curve is intended only as a guide to the eye. Zero-point energy corrections are not included. E^* denotes reaction barrier. ΔE_{rxn} denotes the overall energy change of reaction.

is sufficiently large to allow us to accurately capture the rotational, translational, and bond-stretching components of the reaction coordinate. The experimental saturation coverage (θ_{sat}) for methanol on Cu(110) is 0.36 ML (64) (we were unable to locate any experimental data on saturation coverage for Cu(111)). Assuming a similar θ_{sat} for MeOH on Cu(111), the 3×3 unit cell gives $\theta/\theta_{sat} \approx 0.31$.

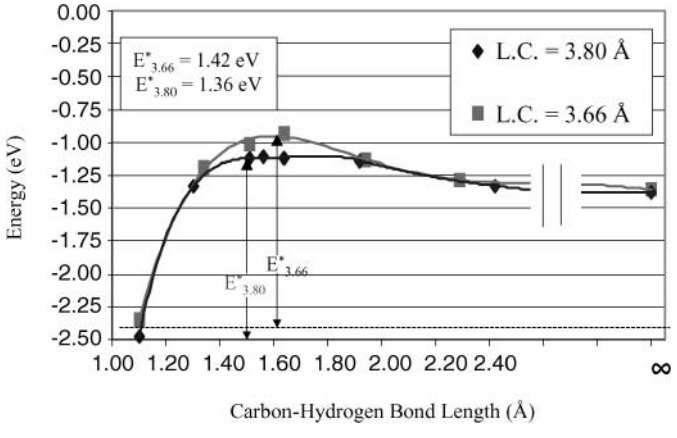

FIG. 3. Reaction coordinate for H-abstraction from methoxy on equilibrium and stretched Cu(111) surfaces. L.C. denotes lattice constant. Zero of energy corresponds to a gas-phase methoxy at infinite separation from the slab. The curves are intended only as guides to the eye. Zero-point energy corrections are not included. E^* denotes reaction barrier. ΔE_{rxn} denotes the overall energy change of reaction.

The initial state is chosen to be the most stable methoxy configuration (fcc). Given the weak site preferences of H and CH_2O on Cu(111), we chose a final state consisting of hydrogen in an hcp site and formaldehyde in the configuration shown in the rightmost snapshot in Fig. 2. The hydrogen essentially moves straight from its initial location on the methoxy radical to its final hcp site, and the formaldehyde group moves up from the surface and rotates to end in its final state almost parallel to the surface. The transition state is formaldehyde-like (Fig. 2), and the calculated reaction barrier is 1.42 eV. Figure 2 also shows the C–O bond length along the reaction path, independently suggesting that the TS is final-state-like. The overall thermochemistry of this reaction step is calculated by analyzing a case of infinite separation between the formaldehyde and the atomic hydrogen products. In this situation, there is no repulsion between the products. The reaction is found to be endothermic by ca. 0.97 eV. We note that the final (coadsorbed) state in the reaction pathway is nearly degenerate with adsorbed formaldehyde and hydrogen at infinite separation from one another (Fig. 2), indicating that there is essentially no interaction between formaldehyde and hydrogen in this coadsorbed state. In addition, since formadehyde lies far from the surface and is weakly bound in all stable adsorption states (Table 1), the specific configuration chosen for this species has little effect on the final state energy and the calculated reaction barrier.

Complete Methanol Decomposition Pathway

The thermochemical and kinetic results for the studied methanol decomposition pathway are summarized in Fig. 4. The thermochemical values presented in the figure are calculated from the highest absolute values of binding energies for all adsorbates involved.

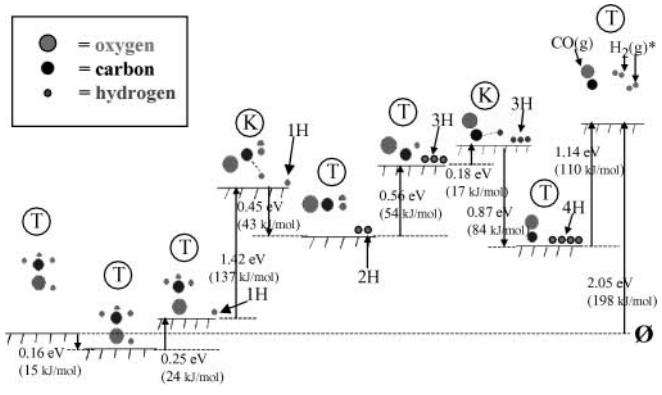

FIG. 4. Schematic potential energy surface for methanol decomposition on Cu(111). Zero of energy corresponds to a gas-phase methanol at infinite separation from the slab. Zero-point energy corrections are not included (for details, see discussion). T denotes a stable intermediate. K denotes a transition state. Successive hydrogen atoms (H) are adsorbed on the surface immediately after their removal from the corresponding intermediates.

DISCUSSION

Structure and Energetics of Adsorbed Intermediates

Some interesting observations can be made about the structure and thermochemistry of the methanol decomposition intermediates on Cu(111). Apparently, atomic hydrogen, methoxy, and, to a lesser extent, formyl, bind very strongly to the Cu(111) surface. This result is not surprising, given that all of these species are radicals and can be expected to be highly reactive. Our calculated binding energies for these intermediates are consistent with previous theoretical work. Cluster studies of *methoxy* adsorption on Cu(111) have produced binding energies of −1.96 (27), −2.82 (33), and −2.39 eV (34), as compared to our value of −2.08 eV at $\theta = 1/9$ ML. The deviation of the cluster values from our slab value is at least partially explained by the different types of calculations (slab vs cluster and different functionals used). Our structural data for methoxy are also consistent with available experimental and theoretical evidence. Experimental investigations with NEXAFS, XPD, HREELS, and ARPS (25–30) have generally concluded that methoxy binds to Cu(111) through the oxygen atom at a hollow site. The adsorbed methoxy is found to be either perpendicular or very slightly off-perpendicular to the surface. The theoretical cluster calculations mentioned above lead to similar conclusions; the fcc site is found to be the most favorable site in these studies, and the methoxy is nearly perpendicular to the surface.

For the *formyl* radical, a cluster calculation gives a binding energy (B.E.) of −1.45 eV (38), which is comparable to our B.E. of −1.15 eV at $\theta = 1/9$ ML. Furthermore, the structural data in the same reference support our result that formyl binds through the carbon atom. For *atomic hydrogen*, a cluster calculation (37) produces a binding energy of −1.71 eV, and a slab calculation yields a B.E. of −2.37 eV at $\theta = 1/3$ ML (45). A value of the B.E. estimated from experimental work is -2.45 ± 0.05 eV (45). The last two values agree reasonably well with our calculated B.E. of −2.37 eV at $\theta = 1/9$ ML. Also, the results in the two theoretical references (37, 45) indicate that the threefold fcc and hcp sites are the most energetically favorable sites for hydrogen, in agreement with our results.

Carbon monoxide binds somewhat less strongly to Cu(111) than do the above radicals. Redhead analyses of TPD data typically give binding energies of -0.52 ± 0.05 eV (41, 42). A DFT slab calculation with CO fixed at a top site yields a binding energy of −0.62 eV (43). These experimental and theoretical values are in fair agreement with our calculated binding energy of −0.79 eV. Although the CO binding energy we calculate agrees fairly well with literature values, it has been demonstrated that DFT methods often give incorrect site preferences for CO on different metals (65). This appears to be the case for CO/Cu(111); we find that fcc is the best site while experiments suggest that on-top adsorption is favored (66).

The thermochemical data indicate that both *methanol* and *formaldehyde* bind very weakly to the clean Cu(111) surface. Binding energies of ca. −0.16 eV for methanol and ca. −0.10 eV for formaldehyde are calculated. The agreement between our results and previously reported binding energies is relatively poor, but the literature values at least confirm that methanol and formaldehyde bind weakly to Cu(111). For *methanol*, a Redhead analysis of SKS data gives a B.E. of about −0.56 eV on Cu(111) (17) and −0.43 eV on Cu(100) (67). For *formaldehyde*, a DFT cluster binding energy of −0.21 eV is found on Cu(111) (37). Also, a value of −0.33 eV (obtained from TPD experiments) is determined on supported copper (18), where adsorption at defect sites is expected to be significant. To examine the effect of defects on formaldehyde adsorption, we have studied formaldehyde binding to a stepped Cu(211) surface. We considered only adsorption at the step edge (in a disigmalike configuration) since terrace binding is expected to be similar to binding on Cu(111). We calculated a B.E. of −0.57 eV, indicating that steps and other defects can account for the supported copper estimated B.E. of −0.33 eV.

The thermochemical pathway presented in Fig. 4 clearly shows the endothermicity of the methanol decomposition reaction and the favorable thermochemistry of the microscopic reverse reaction, methanol synthesis from CO and H_2. The calculated energy change of the overall reaction, 2.05 eV (198 kJ/mol), does not agree well with the experimental value of the standard enthalpy of reaction at 300 K, 0.94 eV (91 kJ/mol) (60). This poor agreement is due, in large part, to the neglect of zero-point energies in our calculations. Correction of our gas-phase energy change for zero-point energy differences (vibrational frequencies, as tabulated in (3, 68), are given in Table 2) yields an overall energy change of 1.38 eV (Table 2), in much better

TABLE 2

Vibrational Frequencies[a] and Zero-Point Energies for Gas-Phase H_2, CO, and CH_3OH

Species	Vibrational frequencies, ν (cm^{-1})	Zero-point energies, E_{zp}[b] (eV)
$H_2(g)$	4405.3	0.273
$CO(g)$	2169.5	0.134
$CH_3OH(g)$	270	0.017
	1033	0.064
	1060	0.066
	1165	0.072
	1345	0.083
	1447 (2)	0.090 (2)
	1455	0.090
	2844	0.176
	2960	0.183
	3000	0.186
	3681	0.228

[a] Ref. (3).
[b] $E_{zp} = 1/2\ h\nu$.

agreement with the experimental value. Correction for finite temperature effects is expected to improve our estimate by another 0.31 eV (yielding an energy change for the overall reaction of 1.07 eV), assuming that the specific heat correlations reported in (69) can be extrapolated to zero temperature. Remaining errors (ca. 0.15 eV) are likely related to errors in the calculation of gas-phase bond energies. For example, the calculated bond energy of CO is 10.95 eV while the accepted experimental enthalpy value at 300 K is 11.16 eV (60).

The data in Fig. 4 demonstrate that, from a purely thermochemical perspective, either the methoxy radical or molecular methanol might be the most abundant surface intermediate in this reaction pathway. For adsorbed methanol, the thermochemistry indicates that desorption is energetically preferable to methoxy formation on *clean*, perfectly flat Cu(111). This result is in agreement with the experimental fact that methanol generally desorbs before decomposing in TPD studies on clean Cu(111) (17). For this reason, studies of methanol decomposition on Cu(111) and other *low-index* copper surfaces (with the exception of Cu(210) (70)) generally rely on preadsorbed oxygen to facilitate methoxy formation (11, 13–17, 71). This process proceeds via the reaction of methanol at the edges of surface oxygen islands (71). After the methoxy formation is completed, the methoxy decomposes to formaldehyde and hydrogen, which quickly desorb as $CH_2O(g)$ and $H_2(g)$ (13–17). This rapid desorption of formaldehyde is explained by our calculations. The calculated binding energy for formaldehyde is only about −0.10 eV while the data in Fig. 4 demonstrate that the reaction barrier for formaldehyde conversion to either methoxy or formyl is at least 0.45 eV. Hence, most formaldehyde that forms will preferentially desorb before further reaction can occur, and formaldehyde is unlikely to be an important surface intermediate in methanol chemistry on copper, in contrast to what has been proposed in a previous microkinetic model (1). Trace amounts of formaldehyde that remain on the surface, however, may react with any oxygen still on the surface, in a minor pathway, to yield formate that subsequently decomposes to give CO_2 and H_2 (13, 15, 17).

It is interesting that in *polycrystalline* studies, formaldehyde can exhibit a behavior different from the above (18, 19). In these studies, the formaldehyde is observed to stick to the surface and to react with oxygen (sometimes present as an impurity in polycrystalline samples (18, 19)) to yield formate, which subsequently decomposes to CO_2 and H_2. The ability of formaldehyde to stick to the surface in these cases could be explained either by an increase in the gas-phase chemical potential of formaldehyde at high pressure or by the stronger binding at surface defects.

The results in Fig. 4 are consistent with the hypothesis that the rate-limiting step (RLS) for methanol *decomposition* is the abstraction of hydrogen from methoxy. Our results by no means prove this idea, as we have not calculated reaction barriers for the remaining elementary steps, but the hypothesis has received support in the experimental literature. Russell *et al.* (17) used kinetic isotope studies to demonstrate that hydrogen abstraction from methoxy is the RLS in the decomposition of methanol to formaldehyde on oxygen-predosed Cu(111). Also, Peppley *et al.* (1) created a microkinetic model of methanol steam reforming based on the assumption that hydrogen abstraction from methoxy is the RLS in this process. Figure 4 is also consistent with the statement that the RLS for methanol *synthesis* from CO may be the hydrogenation of CO to formyl. Our preliminary kinetic analysis of this elementary step indicates that the reaction barrier is about 0.87 eV. This barrier is slightly larger than the desorption energy of CO from Cu(111) (ca. 0.79 eV). Hence, it seems likely that CO will preferentially desorb, rather than hydrogenate to formyl, on Cu(111). This conclusion is in agreement with both a UBI–QEP study performed on Cu(111) (72) and with a high-pressure reactor study (73). In this last study, the investigators found that polycrystalline Cu is inactive toward CO hydrogenation unless potassium promoters are present. In turn, lack of considerable CO hydrogenation to formyl on clean copper is consistent with the idea that CO_2 hydrogenation is the major methanol synthesis pathway on copper (5, 6).

Hydrogen Abstraction from Methoxy

A barrier of 1.42 eV is found for the methoxy hydrogen abstraction step on clean Cu(111). To explore the path dependence of this reaction barrier, a different reaction coordinate between the initial and final states (a path of somewhat lower symmetry) has also been examined. This path, involving movement of the abstracted hydrogen atom over a top site before it resumes its final state, has a similar barrier (ca. 1.40 eV). A further exploration of the path dependence of the reaction barrier was performed by considering the effect of various rotations of the formaldehyde–hydrogen complex (relative to the surface plane) on the reaction barrier. The rotations appeared to contribute an uncertainty of about ±0.1 eV to the barrier. These results suggest that the reaction barrier is not particularly sensitive to the specific hydrogen abstraction path.

The barrier we found is comparable to results obtained by various theoretical and experimental investigations of the methoxy hydrogen abstraction reaction on copper surfaces. Theoretically, DFT cluster calculations predict a barrier of 1.80 eV on Cu(111) (37). Experimentally, Yates and coworkers (17) find that the reaction barrier on *oxygen-predosed* Cu(111) is 1.06 eV. In that experiment, however, the presence of adsorbed oxygen may have lowered the reaction barrier below the barrier for methanol decomposition on clean Cu(111). In a microkinetic study of methanol steam reforming, Peppley *et al.* (1) find barriers of 1.07 and 1.76 eV for the methoxy hydrogen abstraction reaction. They assume that two different types of surface sites

TABLE 3

Effect of Strain on the Thermochemistry of the Abstraction of Hydrogen from the Methoxy Intermediate on Cu(111)

Adsorbate	Methoxy (fcc)	Formaldehyde (top–bridge–top)	Atomic hydrogen (fcc)	Energy change of reaction: $CH_3O^* \rightarrow CH_2O^* + H^*$
B.E. (eV) at 3.66 Å	−2.08	−0.10	−2.37	0.97
B.E. (eV) at 3.80 Å	−2.26	−0.11	−2.45	1.06
Change in energy (eV)	−0.18	−0.01	−0.08	0.09

Note. $\theta = 1/9$ ML. Negative numbers indicate stable intermediates. Energy reference corresponds to adsorbate and slab at infinite separation between each other.

are present in their $Cu/ZnO/Al_2O_3$ study. The first type, possibly decomposition products of a hydroxy–carbonate phase, corresponds to the 1.07-eV value, and the second type, postulated to be elemental copper, corresponds to the 1.76-eV value. The exact nature of these active sites, however, appears to be unclear.

The deviations of our theoretical results from the above experimental results could be caused by many effects. The fact that the activation energy estimated by Yates and coworkers (17) on an oxygen-predosed surface is lower than our calculated value on an oxygen-free surface suggests that adsorbed oxygen may stabilize the methoxy-to-formaldehyde transition state and thereby lower the reaction barrier. Similar effects could also be present in the microkinetic study of Peppley *et al.* (1). Another possible explanation for the observed differences between theory and experiment involves *defect* sites. It is well-known that defects can play a major role in noble metal chemistry (22, 74), and such defects could easily have affected the reaction barriers found in the referred experimental studies.

The above considerations suggest that more detailed models of methanol synthesis catalysts could be useful in explaining experimental results (indeed, we plan to investigate both of the above effects, namely oxygen and defects, in the future). Nonetheless, studies of methanol behavior on Cu(111) can provide useful insights into methanol behavior on industrial methanol synthesis catalysts, as evidenced by recent *in situ* high-pressure HRTEM images showing that a substantial fraction of a methanol synthesis catalyst surface is composed of a Cu(111) plane (75).

An alternative explanation for the experimental and theoretical differences could be the presence of *strain*. Metal oxide catalyst supports (49) or particular kinds of defects (such as dislocations (50)) could certainly introduce strain into the referred experimental surfaces. We find that stretching the bulk-truncated Cu(111) surface by ca. 4% has an effect on the hydrogen abstraction kinetics. Although our calculations show that the reaction barrier only drops from 1.42 to 1.36 eV when the surface is stretched (an amount within the error bars of our calculations—see Fig. 3), the transition state energy drops by ca. 0.15 eV with respect to the gas-phase zero, making hydrogen abstraction from CH_3O more selective than desorption, compared to the selectivity on the equilibrium lattice constant surface.

The effect of strain on the thermochemistry of the methoxy hydrogen abstraction step is found to be small (Table 3). The stretching examined by our calculations stabilizes methoxy (the reactant) by about 0.10 eV more than it stabilizes formaldehyde and hydrogen (the products), corresponding to an increase from 0.97 to 1.06 eV in the calculated energy change of reaction. This amount is almost within the error bars of our calculations, and it can be concluded that strain produces little change in the reaction thermochemistry. Therefore, our limited studies point to improved kinetics as the most likely effect of strain on this reaction.

The above conclusions might confirm, to some extent, the suggestions made by Knop–Gericke *et al.* (20, 21, 23) and Böttger *et al.* (22). These authors propose that strained defect sites on polycrystalline Cu provide a favorable electronic environment for subsurface oxygen atoms. A combination of the Lewis basicity of the subsurface oxygen atoms and the lattice strain induced by these atoms then acts to facilitate the oxidation of adsorbed methanol. We plan to deconvolve these two effects (the effect of strain induced by subsurface oxygen and the electronic effect of subsurface oxygen) in future studies.

CONCLUSIONS

The thermochemistry of the stable intermediates and the reaction barrier of the second elementary step of methanol decomposition (the abstraction of hydrogen from methoxy) on Cu(111) have been studied using periodic self-consistent DFT–GGA calculations. Methanol and formaldehyde are weakly bound on the surface and can easily desorb. CO has a higher binding energy, but it, too, is likely to desorb rather than react. Methoxy, formyl, and atomic hydrogen are all bound quite strongly to the surface; these intermediates will certainly be converted to other intermediates in the decomposition pathway before any desorption occurs.

Our results are consistent with the hypothesis, common in the literature, that the abstraction of hydrogen from methoxy is the RLS in the methanol decomposition pathway. We do not prove this hypothesis, however, as we

did not calculate reaction barriers for all elementary steps involved. Both the thermodynamics and the reaction barrier of the methoxy to formaldehyde step are found to be highly unfavorable. This reaction step is highly endothermic (ca. 1.0 eV), and the corresponding reaction barrier is ca. 1.4 eV. With such unfavorable thermodynamics and kinetics, this step is only significant when the competing reaction, methoxy hydrogenation to methanol, is suppressed (by, for example, removal of surface hydrogen by preadsorbed oxygen). Introduction of an expansive lattice strain tends to lower the energy of the transition state for this step. Future work will focus on the detailed role of oxygen in the decomposition process and on the effect of defect sites on this reaction.

ACKNOWLEDGMENTS

The authors thank Professor J.A. Dumesic for several fruitful discussions. J.G. acknowledges partial financial support from a National Science Foundation predoctoral fellowship and from an NSF Graduate Research Traineeship (Contract EHR-9554586). M.M. acknowledges financial support from an NSF-CAREER Award (CTS-0134561) and a Shell Oil Company Foundation Faculty Career Initiation Award. We thank BP-Amoco for an equipment grant. Both authors acknowledge partial support from NSF cooperative agreement ACI-9619020 through computing resources provided by the National Partnership for Advanced Computational Infrastructure (NPACI). Part of the necessary calculations was performed at the Department of Energy's National Energy Research Scientific Computing Center (NERSC).

REFERENCES

1. Peppley, B. A., Amphlett, J. C., Kearns, L. M., and Mann, R. F., *Appl. Catal. A* **179**, 31 (1999).
2. Thayer, A., *Chem. Eng. News*, Apr. 17 (2000).
3. Askgaard, T. S., Nørskov, J. K., Ovesen, C. V., and Stoltze, P., *J. Catal.* **156**, 229 (1995).
4. Dybkjaer, I., *Chem. Econ. Eng. Rev.* **13**, 17 (1981).
5. Bowker, M., *J. Chem. Soc. Faraday Trans.* **77**, 3023 (1981).
6. Chinchen, G. C., Denny, P. J., Jennings, J. R., Spencer, M. S., and Waugh, K. C., *Appl. Catal.* **36**, 1 (1987).
7. Nerlov, J., and Chorkendorff, I., *Catal. Lett.* **54**, 171 (1998).
8. Rasmussen, P. B., Kazuta, M., and Chorkendorff, I., *Surf. Sci.* **318**, 267 (1994).
9. Mills, P. L., Harold, M. P., and Lerou, J. J., *in* "Catalytic Oxidation: Principles and Applications" (R. A. Sheldon and R. A. van Santen, Eds.), p. 307. World Scientific, New Jersey, 1995.
10. Friend, C. M., and Xu, X., *Annu. Rev. Phys. Chem.* **42**, 251 (1991).
11. Canning, N. D. S., and Madix, R. J., *J. Phys. Chem.* **88**, 2437 (1984).
12. Ellis, T. H., and Wang, H., *Langmuir* **10**, 4083 (1994).
13. Wachs, I. E., and Madix, R. J., *J. Catal.* **53**, 208 (1978).
14. Bowker, M., and Madix, R. J., *Surf. Sci.* **95**, 190 (1980).
15. Sexton, B. A., Hughes, A. E., and Avery, N. R., *Surf. Sci.* **155**, 366 (1985).
16. Madix, R. J., and Telford, S. G., *Surf. Sci.* **328**, L576 (1995).
17. Russell, J. N., Jr., Gates, S. M., and Yates, J. T., Jr., *Surf. Sci.* **163**, 516 (1985).
18. Clarke, D. B., Lee, D. K., Sandoval, M. J., and Bell, A. T., *J. Catal.* **150**, 81 (1994).
19. Fisher, I. A., and Bell, A. T., *J. Catal.* **184**, 357 (1999).
20. Knop-Gericke, A., Hävecker, M., Schedel-Niedrig, T., and Schlögl, R., *Catal. Lett.* **66**, 215 (2000).
21. Knop-Gericke, A., Hävecker, M., Schedel-Niedrig, T., and Schlögl, R., *Top. Catal.* **10**, 187 (2000).
22. Böttger, I., Schedel-Niedrig, T., Timpe, O., Gottschall, R., Hävecker, M., Ressler, T., and Schlögl, R., *Chem.–Eur. J.* **6**, 1870 (2000).
23. Knop-Gericke, A., Hävecker, M., Schedel-Niedrig, T., and Schlögl, R., *Top. Catal.* **15**, 27 (2001).
24. Mavrikakis, M., and Barteau, M. A., *J. Mol. Catal. A* **131**, 135 (1998).
25. Ricken, D. E., Somers, J., Robinson, A. W., and Bradshaw, A. M., *Faraday Discuss. Chem. Soc.* **89**, 291 (1990).
26. Carvalho, A. V., Asensio, M. C., and Woodruff, D. P., *Surf. Sci.* **273**, 381 (1992).
27. Witko, M., Hermann, K., Ricken, D., Stenzel, W., Conrad, H., and Bradshaw, A. M., *Chem. Phys.* **177**, 363 (1993).
28. Hofmann, P., and Menzel, D., *Surf. Sci.* **191**, 353 (1987).
29. Amemiya, K., Kitajima, Y., Yonamoto, Y., Terada, S., Tsukabayashi, H., Yokoyama, T., and Ohta, T., *Phys. Rev. B* **59**, 2307 (1999).
30. Hofmann, P., Schindler, K. M., Bao, S., Fritzsche, V., Ricken, D. E., Bradshaw, A. M., and Woodruff, D. P., *Surf. Sci.* **304**, 74 (1994).
31. Hermann, K., and Meyer, C., *Surf. Sci.* **277**, 377 (1992).
32. Rodriguez, J. A., *Surf. Sci.* **273**, 385 (1992).
33. Witko, M., and Hermann, K., *J. Chem. Phys.* **101**, 10173 (1994).
34. Gomes, J. R. B., and Gomes, J. A. N. F., *J. Mol. Struct.* **463**, 163 (1999).
35. Bryden, T. R., and Garrett, S. J., *J. Phys. Chem. B* **103**, 10481 (1999).
36. Gomes, J. R. B., Gomes, J. A. N. F., and Illas, F., *J. Mol. Catal. A* **170**, 187 (2001).
37. Gomes, J. R. B., Gomes, J. A. N. F., and Illas, F., *Surf. Sci.* **443**, 165 (1999).
38. Gomes, J. R. B., and Gomes, J. A. N. F., *J. Electroanal. Chem.* **483**, 180 (2000).
39. Yang, H., *Surf. Sci.* **343**, 61 (1995).
40. Yates, J. T., Jr., and Cavanagh, R. R., *J. Catal.* **74**, 97 (1982).
41. Kirstein, W., Krüger, B., and Thieme, F., *Surf. Sci.* **176**, 505 (1986).
42. Bönicke, I., Kirstein, W., Spinzig, S., and Thieme, F., *Surf. Sci.* **313**, 231 (1994).
43. Hammer, B., Morikawa, Y., and Nørskov, J. K., *Phys. Rev. Lett.* **76**, 2141 (1996).
44. Kammler, T., and Küppers, J., *J. Chem. Phys.* **111**, 8115 (1999).
45. Strömquist, J., Bengtsson, L., Persson, M., and Hammer, B., *Surf. Sci.* **397**, 382 (1998).
46. Pallassana, V., Neurock, M., Hansen, L. B., and Nørskov, J. K., *J. Chem. Phys.* **112**, 5435 (2000).
47. Hrbek, J., de la Figuera, J., Pohl, K., Jirsak, T., Rodriguez, J. A., Schmid, A. K., Bartlelt, N. C., and Hwang, R. Q., *J. Phys. Chem. B* **103**, 10557 (1999).
48. Bennett, R. A., Poulston, S., Price, N. J., Reilly, J. P., Stone, P., Barnes, C. J., and Bowker, M., *Surf. Sci.* **433–435**, 816 (1999).
49. Giorgio, S., Henry, C. R., Pauwels, B., and van Tendeloo, G., *Mater. Sci. Eng. A* **297**, 197 (2000).
50. Wintterlin, J., Zambelli, T., Trost, J., Mavrikakis, M., and Greeley, J. P., submitted for publication.
51. Gsell, M., Jakob, P., and Menzel, D., *Science* **280**, 717 (1998).
52. Mavrikakis, M., Hammer, B., and Nørskov, J. K., *Phys. Rev. Lett.* **81**, 2819 (1998).
53. Gunter, M. M., Ressler, T., Bems, B., Buscher, C., Genger, T., Hinrichsen, O., Muhler, M., and Schlögl, R., *Catal. Lett.* **71**, 37 (2001).
54. Hammer, B., Hansen, L. B., and Nørskov, J. K., *Phys. Rev. B* **59**, 7413 (1999).
55. Neugebauer, J., and Scheffler, M., *Phys. Rev. B* **46**, 16067 (1992).
56. Vanderbilt, D. H., *Phys. Rev. B* **41**, 7892 (1990).
57. Perdew, J. P., Chevary, J. A., Vosko, S. H., Jackson, K. A., Pederson, M. R., Singh, D. J., and Fiolhais, C., *Phys. Rev. B* **46**, 6671 (1992).
58. White, J. A., and Bird, D. M., *Phys. Rev. B* **50**, 4954 (1994).
59. Kresse, G., and Forthmüller, J., *Comput. Mater. Sci.* **6**, 15 (1996).

60. "CRC Handbook of Chemistry and Physics" (David R. Lide and H. I. R. Frederikse, Eds.), 76th Ed. CRC Press, New York, 1996.
61. Ulitsky, A., and Elber, R., *J. Chem. Phys.* **92**, 1510 (1990).
62. Mills, G., Jonsson, H., and Schenter, G. K., *Surf. Sci.* **324**, 305 (1995).
63. Greeley, J., and Mavrikakis, M., *J. Am. Chem. Soc.*, accepted for publication.
64. Peremans, A., Maseri, F., Darville, J., and Gilles, J.-M., *J. Vac. Sci. Technol. A* **8**, 3224 (1990).
65. Feibelman, P. J., Hammer, B., Nørskov, J. K., Wagner, F., Scheffler, M., Stumpf, R., Watwe, R., and Dumesic, J., *J. Phys. Chem. B* **105**, 4018 (2001).
66. Hayden, B. E., Kretzschmar, K., and Bradshaw, A. M., *Surf. Sci.* **155**, 553 (1985).
67. Sexton, B. A., and Hughes, A. E., *Surf. Sci.* **140**, 227 (1984).
68. Ovesen, C. V., Stoltze, P., Nørskov, J. K., and Campbell, C. T., *J. Catal.* **134**, 445 (1992).
69. Kyle, B. G., "Chemical and Process Thermodynamics," 2nd ed., p. 545. Prentice Hall, Englewood Cliffs, NJ., 1992.
70. Chen, A. K., and Masel, R., *Surf. Sci.* **343**, 17 (1995).
71. Leibsle, F. M., Francis, S. M., Haq, S., and Bowker, M., *Surf. Sci.* **318**, 46 (1994).
72. Shustorovich, E., and Bell, A. T., *Surf. Sci.* **253**, 386 (1991).
73. Sheffer, G. R., and King, T. S., *J. Catal.* **115**, 376 (1989).
74. Somorjai, G. A., "Introduction to Surface Chemistry and Catalysis." Wiley, New York, 1994.
75. Hansen, P. L., Wagner, J. B., Helveg, S., Rostrup-Nielsen, J. R., Clausen, B. S., Topsøe, H. T., *Science* **295**, 2053 (2002).